International Journal of Hybrid Information Technology
Vol. 9, No. 6 (2016), pp. 231-244
http://dx.doi.org/10.14257/ijhit.2016.9.6.20

Modeling and Emulation of 3d Dither Stability in Orthogonal Turn-Milling

Yueqi Guan[1]*, Hanqing Guan[2], Gaoshen Wang[1] and Rongling Chen[3]

[1]*Department of Mechanical Engineering, Hunan Institute of Engineering, 411101, Xiangtan, China*
[2]*School of Mechanical Engineering, Xiangtan University, 411105, Xiangtan, China*
[3]*Xiangtan Electric Manufacture Group Co. Ltd., 411101, Xiangtan, China*
383174624@qq.com

Abstract

Aiming at 4-axial orthogonal turn-milling by end mill, its theoretical 3d model for stable range of dither was put forward on the basis of its cutting principle by using analytical method. Based on modal trial, the stable range leaf figure of end mill's dither in 4-axial turn-milling with eccentricity was simulated and analyzed. The results show that besides geometrical shape of mill, material of workpiece and frequency response function of machine-tool's structure etc that can produce dither in 4-axial turn-milling, the rotating speed of mill and cutting depth are also related to dither. In trial of 4-axial turn-milling by end mill, the results of cutting force spectrum analysis show that: cutting is stable and un-dither when frequency of cutter tooth cutting-in plays leading role in force spectrum. Dither is produced when modal frequency of system plays leading role in force spectrum, the measured value of cutting force and surface roughness are also higher than those in the condition of un-dither. Thus the theoretical model and results of emulation can predict stability of end mill's dither in 4-axial orthogonal turn-milling with eccentricity correctly and can provide theoretical guidance for surface quality and processing efficiency of workpiece.

Keywords: *end mill, 4-axial turn-milling, dither stability, eccentricity processing, modeling, emulation*

1. Introduction

Orthogonal turn-milling is the most important processing method in 4-axial milling and is widely used. Orthogonal turn-milling realize processing by using resultant rotating movement of mill and workpiece. The 4-axial orthogonal turn-milling use the multi-blade cutter such as end mill which is cutting interruptedly, thus it can get better chip, higher removal rate of metal and can remove chip easily. It is especially suitable for rough machining of heavy solid of revolution such as large roller, large generator rotor and large mould of cast tube. Its cutting speed is the resultant velocity of cutter and workpiece, so it can realize high-speed cutting without high-speed rotating of workpiece that is good for high-speed cutting of large workpiece. It is suitable for finish machining of axial part which is long and thin because of rotating speed of workpiece is relatively low[1].

The 4-axial orthogonal turn-milling by end mill with eccentricity is an advanced machining method that its working accuracy and working efficiency etc can achieve practical requirements [2-3]. Not only the 4-axial orthogonal turn-milling by end mill has the cutting property of variable cutting depth and thickness because of the resultant movement of mill and workpiece rotating simultaneously, but also it may produce chatter marks on the surface of workpiece and reduce the surface quality of finished surface for the reason of using the multi-blade cutter. For the sake of studying boundary conditions of un-dither stable range in 4-axial orthogonal turn-milling by end mill, the study of dither stability in 4-axial orthogonal turn-milling by end mill with eccentricity has very important theoretical significance and value of practical application [4-7].

At present many scholars at home and abroad are studying mainly on dither stability in turning or milling which has two degree of freedom, however the study on dither stability in turn-milling is relatively small. References [8-9] studied 3d dither stability on the basis of structural particularity of ball end mill. They put forward that stable range leaf figure of ball end mill was acquired by analytic solution in the frequency domain, so the removal rate of cutting and working accuracy of ball end mill were improved effectively. SHAMOTO *etc.*, [10] established model of 3d cutting force and mainly studied by analyzing the dither stability with the consideration of cutting edge inclination of ball end mill during milling. POGACNIK *etc.*, [11] studied on dynamic stability in turning and results showed that vibration had significant influence on surface quality. Optimization of cutting parameters could effectively avoid instability of turning. SCHUBERT *etc.*, [12] found that wear-resisting cutter could realize the machining of difficult-to-machine materials by studying the trial of high-speed turning. Better surface quality could be acquired by avoid range of instability.

Domestic scholars SONG *etc.*, [13-15] studied dither stability in milling by theoretical modeling and optimization on the different cutting condition. LIU Zhanqiang *etc.*, [16] summarized diagrams and theories of 3d dither stability in milling at home and abroad. They put forward that the influence of main shaft's speed, axial cutting depth and radial cutting depth to stability of milling should be studied for the sake of ensuring the maximum removal rate of materials. SHI Li *etc.*, [17] studied the vibration signal in the trial of machining aluminum alloy thin-wall solid of revolution in orthogonal turn-milling and avoided sensitive range of dither by adjusting the speed of rotating. All these studies have laid the foundation for study of dither stability in turn-milling by end mill. For the past few years many professors and scholars [18-19] restrained dither in machining by using ultrasonic vibration, but it was mainly used for machining brittle materials or precise machining. In the study of 3d dither stability in 4-axial turn-milling by end mill, not only the removal efficiency of materials should be enhanced, the surface quality should be enhanced as well. Especially when machining the solid of revolution, larger cutting depth is required to enhance the removal efficiency of materials. It is significant for the study of 3d dither stability in 4-axial orthogonal turn-milling by end mill with eccentricity because of the interaction of cutting force in x, y, z three direction.

2. Modeling of 3d Dither in Orthogonal 4-axial turn-milling by End Mill

As is shown in Figure 1, the rotating axis of mill in orthogonal 4-axial turn-milling is vertical to rotating axis of workpiece. A typical orthogonal turn-milling consists of rotate movement of workpiece, rotate movement of mill and linear feed movement of mill. Because the machining objects mainly are large solid of revolution and slender shaft parts, linear feed movement of mill is often axial feed movement and radial feed movement is rarely used in orthogonal turn-milling.

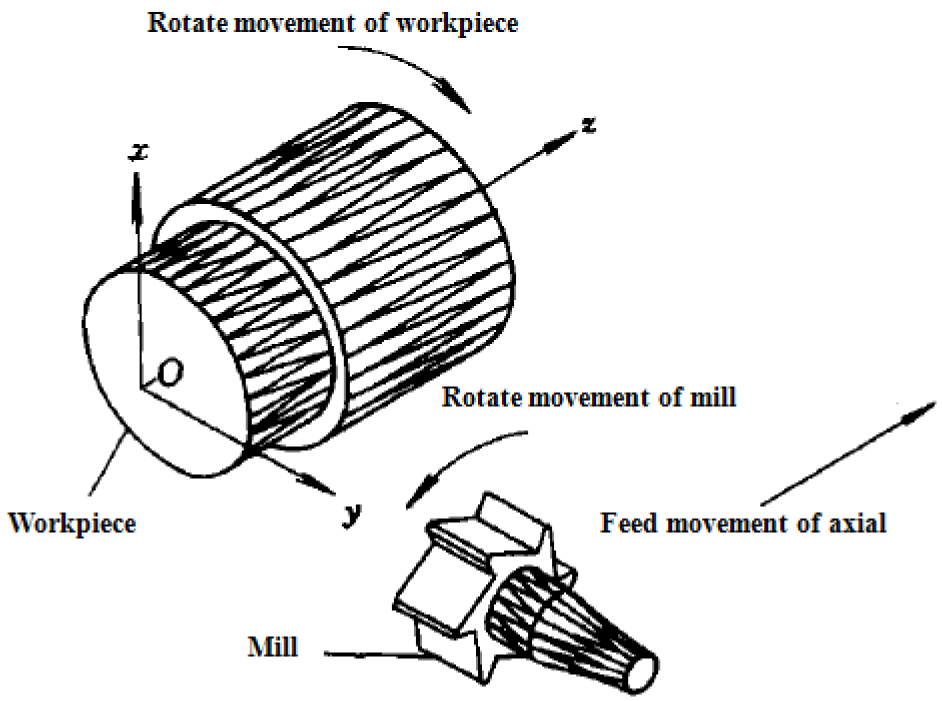

Figure 1. Mainly Movements in Orthogonal 4-axial Turn-Milling

In machining of orthogonal 4-axial turn-milling by end mill, because of interaction of cutting force in end mill and workpiece, analysis of cutting force in three directions are shown in Figure 2. Supposing that the number of cutter tooth on end mill is N which its helical angle is 0°, the dynamic displacements which are produced by cutting force are respectively x , y and z in the direction of feed direction(X), normal direction(Y) and axial direction of main shaft(Z). The dynamic displacement of current cutter tooth j can be expressed by:

$$v_j = (x \sin \phi_j + y \cos \phi_j) \cos \alpha - z \sin \alpha \tag{1}$$

In the expression: Φ_j-Instant contact angle of cutter tooth j which is measured clockwise from normal axis (Y).

α-Angle between direction of cutting thickness $\delta_p(\Phi_j)$ in side edge and direction of cutting thickness $\delta_f(\Phi_j)$ in end edge.

$$\alpha = \arccos \frac{\delta_f(\phi_j)}{\delta_p(\phi_j)} = \frac{\left[r \cos \phi_j - e + \left(R - a_{pp} \right) \tan \dfrac{\Delta \theta_z}{2} \right] \tan \left(\Delta \theta_z \right)}{- f_z \cos \left(\phi_j + \gamma \right)} \tag{2}$$

In the expression: R-Radius of workpiece.

r-Radius of end mill.

α_{pp}-Cutting depth.

f_z-Feed per tooth.

e-Eccentricity.

γ-Angle between original coordinate and rotational coordinate.

$\Delta\theta_z$-Angle of rotation between workpiece and two adjacent cutter tooth.

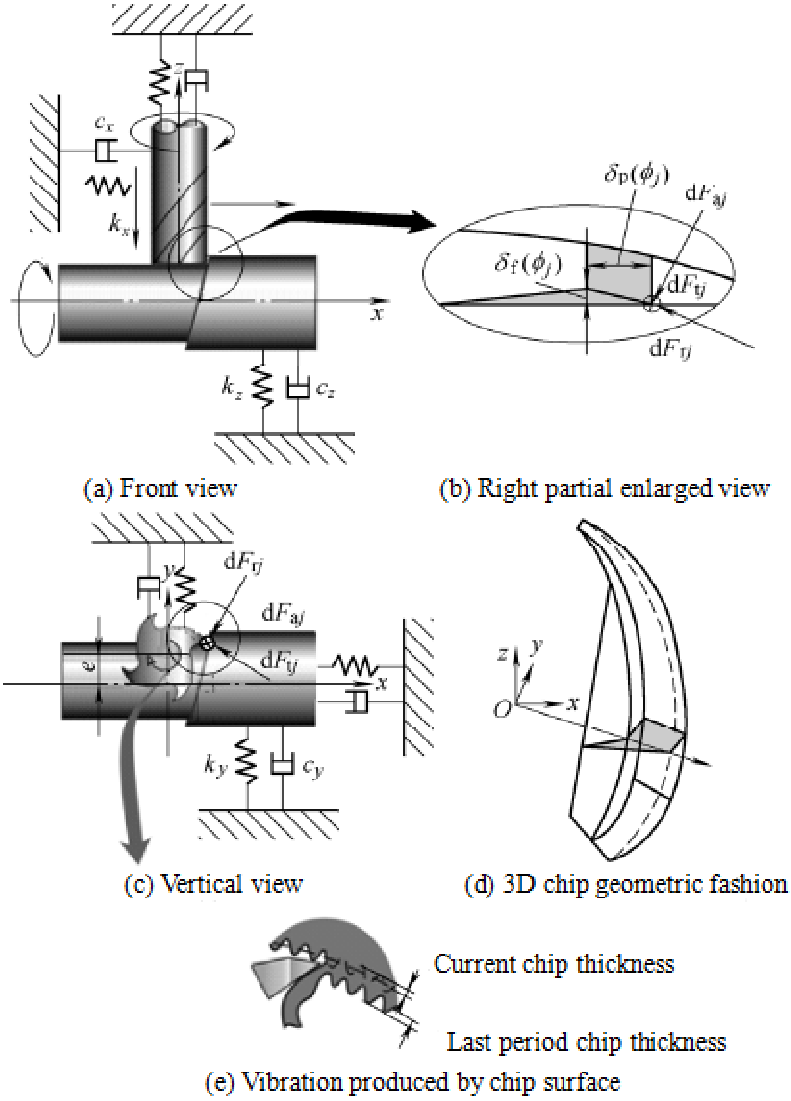

Figure 2. The 3d Shape of Chip when End Mill and Workpiece Vibrating Relatively in Three Direction

As is shown in Figure 2, k_x, k_y, k_z is the stiffness coefficient of end mill and workpiece system in direction of x, y, z respectively. c_x, c_y, c_z is the damping coefficient of end mill and workpiece system in direction of x, y, z respectively. dF_{aj}, dF_{rj}, dF_{tj} is the stressed unit of the j cutting edge in direction of axial direction, radial direction and tangential direction respectively.

If the angular speed of end mill is ω_1, the relationship between contact angle and time is $\phi_j = \omega_1 t$. The final cutting thickness consists of two parts, one is the static cutting thickness caused by rigid movement of end mill, the other is the changing dynamic cutting thickness caused by vibration between current cutter tooth and forward cutter tooth. So the total cutting thickness can be expressed by[8]:

$$\delta(\phi_j) = \left[\delta_s(\phi_j) + \left(v_{j,1} - v_j\right)\right] g(\phi_j) \tag{3}$$

In the expression: $v_{j,1}$-Dynamic displacement of the forward cutter tooth.
$g(\Phi_j)$-Unit step function which is used for ensuring whether the cutter tooth is in cutting.

$$g(\phi_j) = 1 \quad \Phi_{pst}<\Phi_j<\Phi_{pex}$$

$g(\phi_j) = 0 \quad \Phi_{pst} < \Phi_j$ or $\Phi_j > \Phi_{pex}$

Φ_{pst}, Φ_{pex}-Angle of cutting-in and cutting-away.

Because the static cutting thickness has no influence on dynamic cutting thickness which can produce regenerative vibration, it won't exist in the expression. The expression of dynamic cutting thickness is:

$$\delta_d(\phi_j) = \left(\Delta x \sin \phi_j + \Delta y \cos \phi_j \cos \alpha - \Delta z \sin \alpha\right) g(\phi_j) \tag{4}$$

In the expression: Δx-Dynamic displacement in x direction between the period of current cutter tooth and forward cutter tooth.

$\Delta x = x(t) - x(t - T)$

t-Time of cutting.

T-Time of cutting between current cutter tooth and forward cutter tooth.

Δy-Dynamic displacement in y direction between the period of current cutter tooth and forward cutter tooth.

$\Delta y = y(t) - y(t - T)$

Δz-Dynamic displacement in z direction between the period of current cutter tooth and forward cutter tooth.

$\Delta z = z(t) - z(t - T)$

According to expression (4): Tangential cutting force F_{tj}, radial cutting force F_{rj} and axial cutting force F_{aj} on cutter tooth j are in direct proportion to axial cutting depth a_{pp} and cutting thickness δ_d.

$$\begin{bmatrix} dF_r \\ dF_t \\ dF_a \end{bmatrix} = K_t a_{pp} \begin{bmatrix} K_r \\ 1 \\ K_a \end{bmatrix} (\sin \phi \sin a \cos \phi \cos \alpha - \sin \alpha) \times \begin{bmatrix} \Delta x \\ \Delta y \\ \Delta z \end{bmatrix} g(\phi_j) \tag{5}$$

In the expression: K_t, K_a and K_r is coefficient of cutting force in tangential direction, axial direction and radial direction respectively.

Decomposing the cutting force into x, y and z three direction:

$$\begin{bmatrix} dF_x \\ dF_y \\ dF_z \end{bmatrix} = \begin{bmatrix} -\cos \alpha \sin \phi & -\cos \phi & \sin \alpha \sin \phi \\ -\cos \alpha \cos \phi & \sin \phi & \sin \alpha \cos \phi \\ -\sin \alpha & 0 & -\cos \alpha \end{bmatrix} \times \begin{bmatrix} dF_r \\ dF_t \\ dF_a \end{bmatrix} \tag{6}$$

Adding the cutting force on all cutter tooth, total cutting force on end mill is:

$$\begin{cases} F_x = \sum_{j=0}^{N-1} F_{xj}(\phi_j) \\ F_y = \sum_{j=0}^{N-1} F_{yj}(\phi_j) \\ F_z = \sum_{j=0}^{N-1} F_{zj}(\phi_j) \end{cases} \tag{7}$$

The matrix form can be acquired by expression of cutting thickness and expression of cutting force in cutter tooth.

$$\begin{bmatrix} F_x \\ F_y \\ F_z \end{bmatrix} = K_t a_{pp} A \begin{bmatrix} \Delta x \\ \Delta y \\ \Delta z \end{bmatrix} \tag{8}$$

In the expression: A is the directional dynamic matrix of cutting force coefficient which is time-varying.

The expression (8) can be expressed as matrix form in time domain:

$$F(t) = K_t a_{pp} A(t)(\Delta x \quad \Delta y \quad \Delta z)^T \tag{9}$$

$$A_0 = \frac{1}{T}\int_0^T A(t)dt = \frac{1}{\phi_p}\int_{\phi_{pst}}^{\phi_{pex}} A(\phi_j)d\phi_j \tag{10}$$

In the expression: A_0-Directional matrix of cutting coefficient which is not time-varying but depends on contact angle.

Φ_p-Tooth spacing angle of mill

Because the average cutting force is irrelevant to helical angle in each cutter tooth during cutting period, A_0 is suitable for helical end mill. As is shown in Figure 3, physical analysis reveals that higher harmonics in function of cutting force are filtered by low-pass during machining. If dither is existed in 4-axial turn-milling by end mill, the main dither frequency of regenerative vibration spectrum is ω_c.

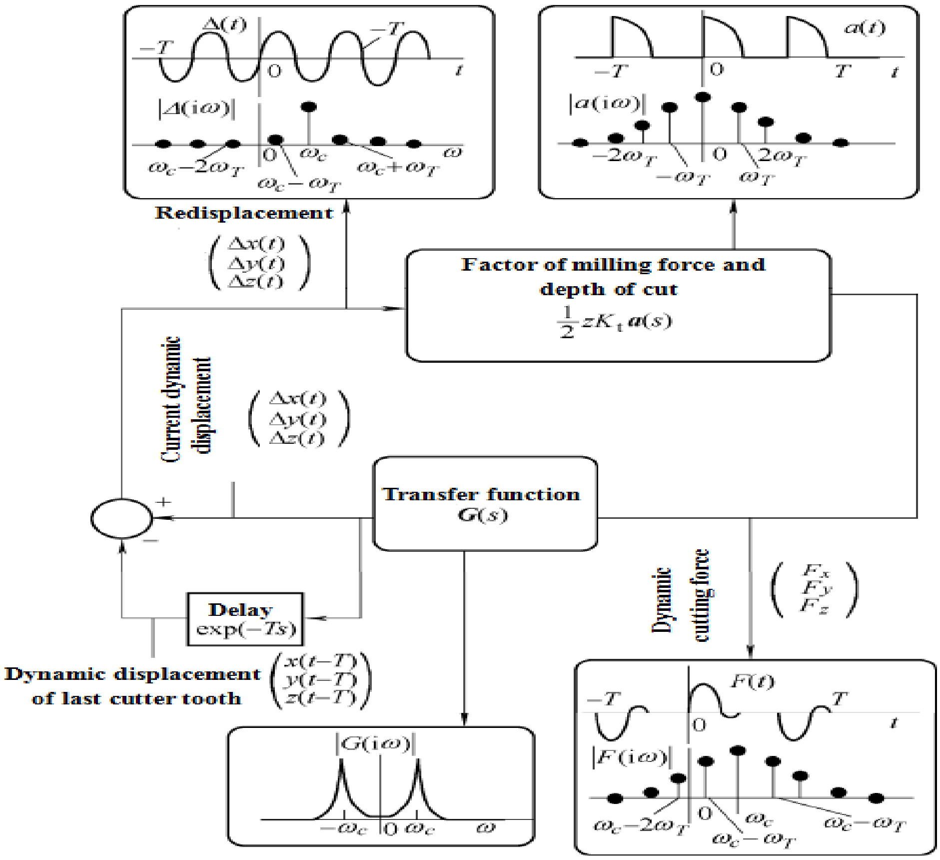

Figure 3. The Regenerative Dither in Turn-Milling by End Mill during Machining

In Figure 3, G(s) is the transfer function, ω_T is the cutting frequency of cutter tooth in harmonic, a(s) is the integral function of directional cutting coefficient and Z is the factor of complex variable. $\Delta(t)$ is the composite renewable displacement in direction of x, y and z. F(t) is the composite dynamic cutting force in direction of x, y and z. F_x, F_y and F_z is the dynamic cutting force in direction of x, y and z.

$$G(s)=\begin{bmatrix} G_{xx}(s) & G_{xy}(s) & G_{xz}(s) \\ G_{yx}(s) & G_{yy}(s) & G_{yz}(s) \\ G_{zx}(s) & G_{zy}(s) & G_{zz}(s) \end{bmatrix}$$

$$a(s)=\begin{bmatrix} a_{xx}(s) & a_{xy}(s) & a_{xz}(s) \\ a_{yx}(s) & a_{yy}(s) & a_{yz}(s) \\ a_{zx}(s) & a_{zy}(s) & a_{zz}(s) \end{bmatrix}$$

The vector of vibration at current moment (t) is $r_0=(x(t),y(t),z(t))^T$, the vector of vibration in forward cutting period (t-T) is $r_1=(x(t-T),y(t-T),z(t-T))^T$. Thus, the produced vector of vibration is:

$$\Delta(t)=r_0(i\omega_c)-r_1(i\omega_c)=[1-\exp(-i\omega_c T)]\exp(i\omega_c t)G(i\omega_c)F(t) \tag{11}$$

In the expression, G(iω) is the matrix of transfer function in contact range of cutter and workpiece.

$$G(i\omega)=\begin{bmatrix} G_{xx}(i\omega) & G_{xy}(i\omega) & G_{xz}(i\omega) \\ G_{yx}(i\omega) & G_{yy}(i\omega) & G_{yz}(i\omega) \\ G_{zx}(i\omega) & G_{zy}(i\omega) & G_{zz}(i\omega) \end{bmatrix} \tag{12}$$

The current cutting force can be expressed by:

$$F(i\omega_c)\exp(i\omega_c t)=\frac{N}{2\pi}K_t a_{pp}A_0[1-\exp(-i\omega_c T)]\times G(j\omega_c)F(i\omega_c)\exp(i\omega_c t) \tag{13}$$

The characteristic value in characteristic equation is:

$$\Lambda=\frac{N}{4\pi}a_{pp}K_t[1-\exp(-i\omega_c T)] \tag{14}$$

Putting the characteristic value and $\exp(-i\omega_c T)=\cos\omega_c T-i\sin\omega_c T$ into equation, the critical cutting depth of dither frequency ω_c is:

$$a_{pm}=-\frac{2\pi\Lambda_R}{NK_t}(1+k^2)=-\frac{2\pi\Lambda_R}{NK_t}\left\{1+\left[\frac{\sin\omega_c T}{(1-\cos\omega_c T)}\right]^2\right\} \tag{15}$$

In the expression: k-The integer number of oscillation mark when cutting arc.
Λ_R-The real part of characteristic value.

$$\omega_c T=\pi-2\phi+2k\pi=\varepsilon+2k\pi$$

Rotating speed of main shaft can be acquiring by the acquired cutting period of cutter:

$$T=\frac{1}{\omega_c}(\varepsilon+2k\pi) \tag{16}$$

Thus:

$$n=\frac{60}{NT}$$

3. Emulation and Trial Result's Analysis of Dither's Stable Range in Orthogonal 4-axial Turn-Milling by End Mill

Methods of studying the stable range of dither in orthogonal 4-axial turn-milling by end mill with eccentricity is acquiring the modal parameters by trial of excitation, then simulating the response function of frequency and stable range leaf figure of dither respectively, the theoretical model and results of emulation are verified by trial. The trial of excitation is shown in Figure 4.

Figure 4. Trial of Excitation

The equipments of trial are as follows: Trialing of excitation and dither stability are on the 4-axial linkage machining center NV610. Model of hilt is KENNAMETAL DV30ER25060, model of end mil is the Chengdu EAGLE: ZE12.21.4—30 with 4 cutting edges and its diameter is 12mm. Material of workpiece is duralumin 2A12 and its diameter is 60mm. Model of acquisition box is USB-9162 Carrier I/O, model of force sensor is C129289(2.13 mV/N), model of acceleration sensor is 3225F1(Sensitivity: 10.00 mV/g), model of displacement sensor is PHILTEC Model RC20. Trial of dither stability in machining is shown in Figure 5.

Figure 5. Trial of Dither Stability in Orthogonal 4-axial Turn-Milling by End Mill

Because the feature of modal matrix and symmetry of transfer function, the modal parameters in table 1 in three directions are G_{xy} =G_{yx}, G_{xz} =G_{zx}, G_{yz} =G_{zy}. The transfer function of original point is the function G_{xx}, G_{yy} and G_{zz} which are measured by using impact hammer impacts at the point installing the accelerometer. The cross transfer function is the function G_{xy}, G_{xz} and G_{yz} which are measured by using impact hammer impacts at the point different from the point installing the accelerometer. These frequencies are the inherent frequency of system, then the data is curve-fitting by polynomial of order (n*n). Thus the value of inherent frequency, damping and stiffness in each mode is estimated.

Table 1. The Modal Parameters of Mill in Three Directions

Transfer function	Inherent frequency f/Hz	Dimension-Damping c	stiffness k/(MN·m^{-1})
G_{xx}	1466.1	0.0344	52.03
	4261.4	0.0335	190.39
G_{yy}	1483.4	0.0219	95.15
	4244.9	0.0248	269.42
G_{zz}	1501.1	0.0226	306.03
	1733.7	0.0257	1557.09
	4356.8	0.0348	583.69
G_{xy}	1476.1	0.0361	48.79
	4267.5	0.0278	201.99
G_{xz}	1471.8	0.0328	503.66
	4442.0	0.0306	1056.95
G_{yz}	1493.6	0.0352	559.66
	4251.1	0.0302	127.88

Figure 6-8 is the transfer function of original point in the knifepoint of end mill in the direction of x, y and z respectively. The comparing figure of trial curve and curve of emulation in the initial conditions of modal parameters, its results can predict the response function of practical knifepoint and provide conditions for emulation and analysis of dither. Scanning the total frequency of main mode in transfer function which its real part is negative.

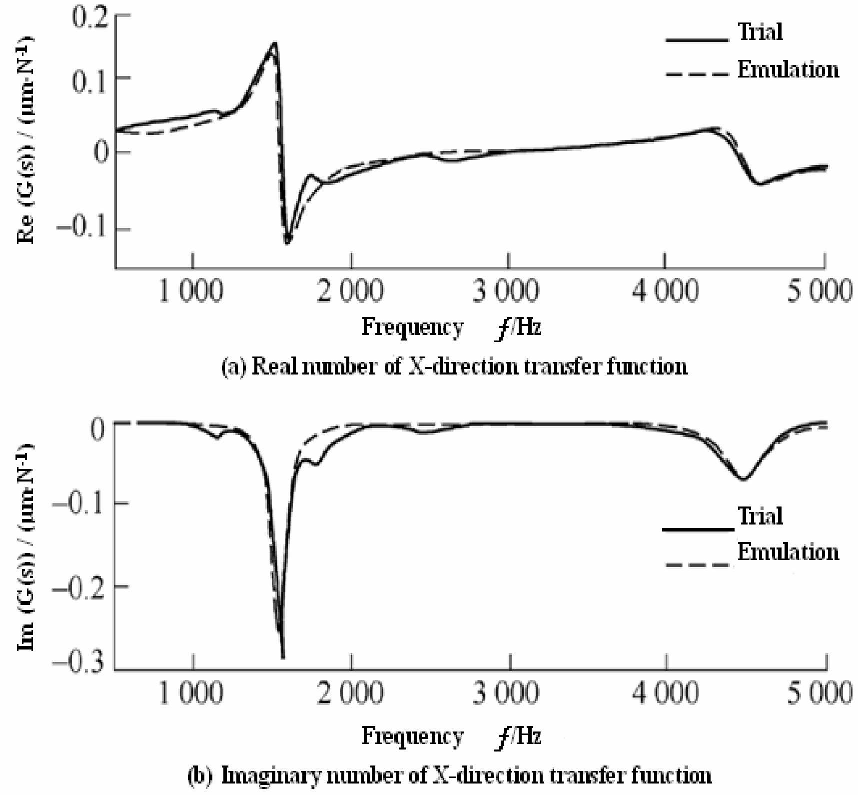

Figure 6. Transfer Function of Mill's Knifepoint in x Direction

Because the coefficient of cutting force is relevant to wear of cutter, it has to be measured before the trial of dither stability in orthogonal 4-axial turn-milling by end mill, regardless of the wear degree of cutter. Coefficient of cutting force reflects in stable range leaf figure of dither, so wear of cutter influences the shape of leaf figure indirectly. The predicting stable range leaf figure of dither is quite accurate when wear of cutter is relatively small. Coefficient of cutting force has to be re-measured and stable range of dither has to be re-ensured with the increasing of the wear of cutter. Thus, the coefficient of cutting force has to measured according to wear of cutter in order to ensure the accuracy of predicting the stable range of dither in orthogonal 4-axial turn-milling by end mill.

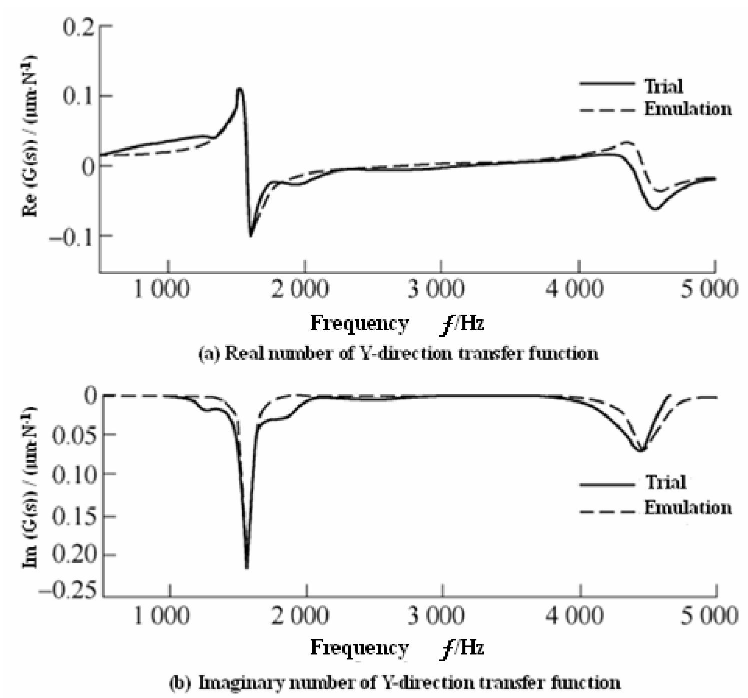

Figure 7. Transfer Function of Mill's Knifepoint in y Direction

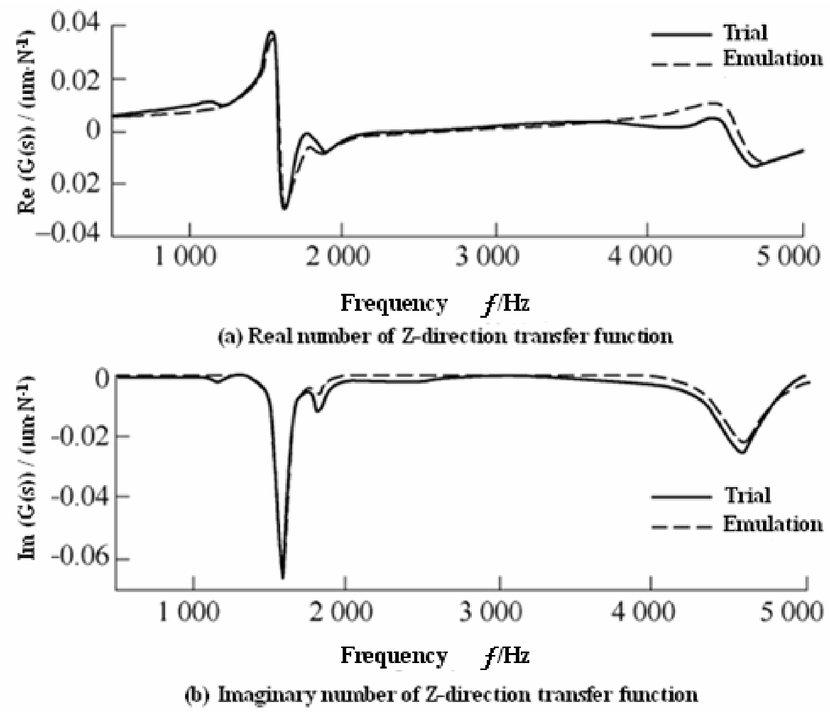

Figure 8. Transfer Function of Mill's Knifepoint in z Direction

Figure 9 shows the stable range leaf figure of dither and results of analysis in orthogonal 4-axial turn-milling by end mill. Figure 9a is the 3d stable range leaf figure of dither in turn-milling by end mill with eccentricity. As is shown in Figure 9a, the dither exist in the leaf and the ranges of outside leaf and below leaf are un-dither during machining. Figure 9b, 9e and 9g is the surface quality, cutting force and spectrum analysis of 1st point in workpiece respectively. Figure 9d, 9f and 9h is the surface quality, cutting force and spectrum analysis of 3rd point in workpiece respectively. In Figure 9a, the cutting depth is 2mm and rotating speed of end mill is 2400rpm at the position of point 1 in the figure. There is severe dither exists which can be observed in trial and can be verified by force spectrum. Dither occurs at frequency of 1608Hz which is close to 1st modal of system. There is slight dither exists at the 2nd point where the cutting depth is 2mm and rotating speed of end mill is 2700rpm in Figure 9a. There is un-dither the 3rd point where the cutting depth is 2mm and rotating speed of end mill is 3600rpm in figure 9a. The force spectrum shows that forced vibration frequency of main shaft or forced vibration cutting frequency of cutter tooth is around 240Hz or its integral multiple. In order to avoid dither, the stability of machining can be predicted by different cutting depth and rotating speed of main shaft. However, there is still some slight dither in stable range leaf figure of dither, so the model of 3d stable range of dither needs to be optimized properly.

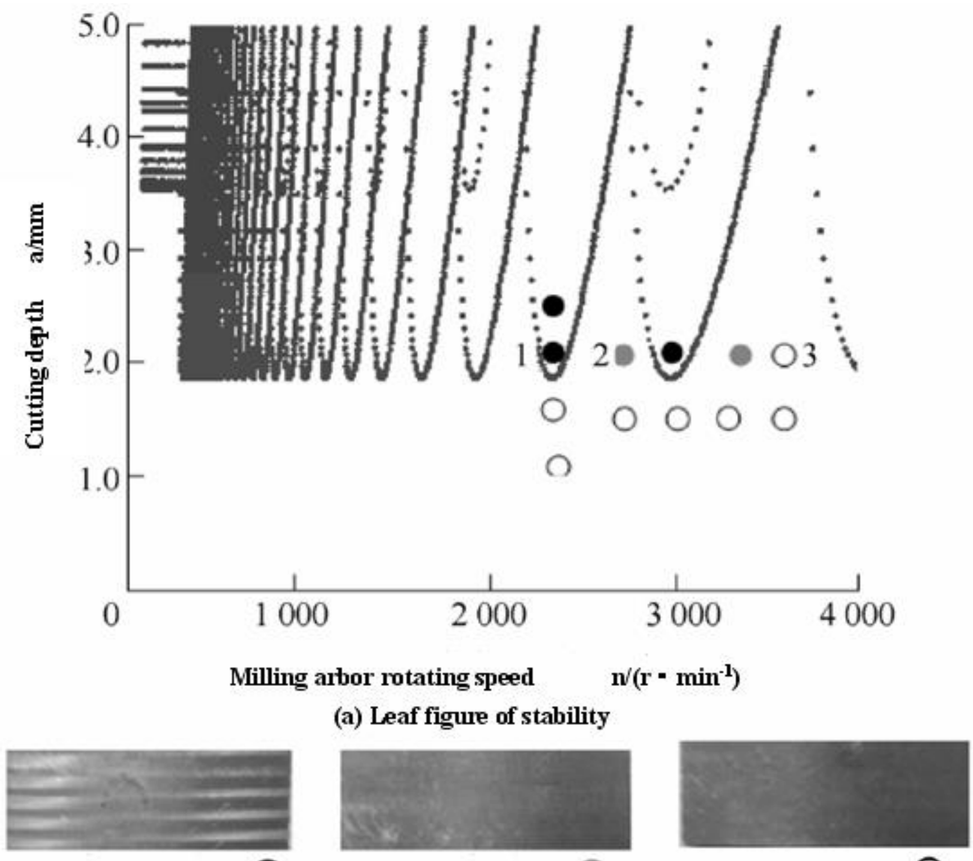

(a) Leaf figure of stability

(b) Skin of dither ● (c) Skin of micro-dither ● (d) Skin of un-dither ○

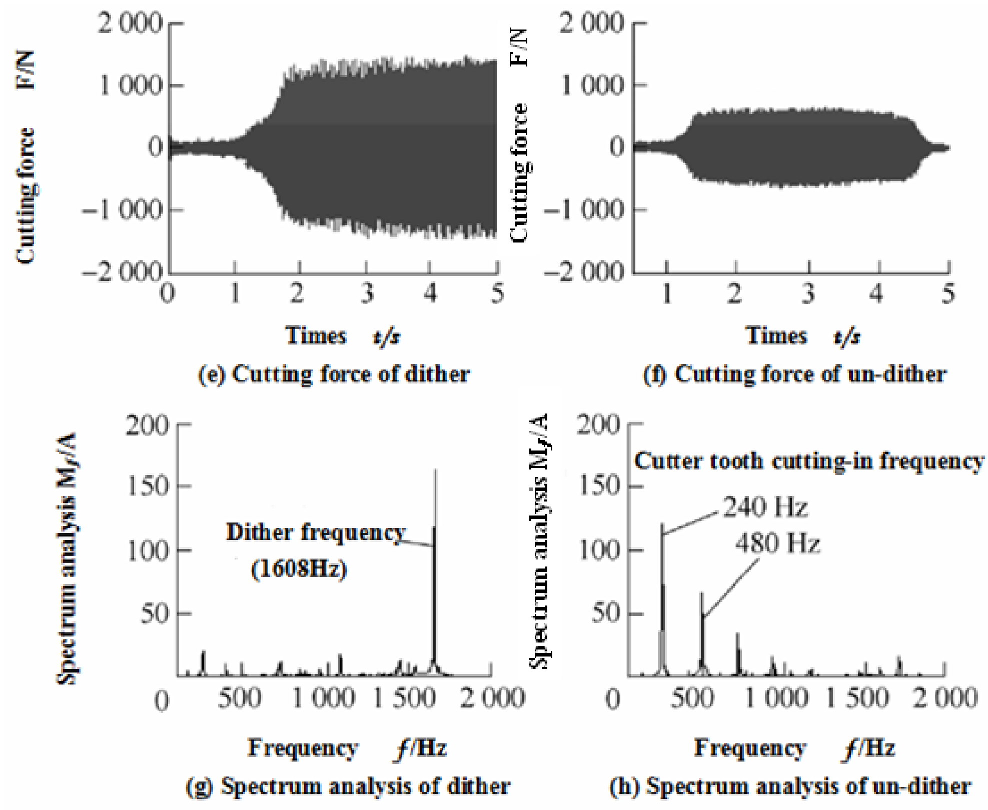

Figure 9. The Stable Range Leaf Figure of Dither and Results of Analysis in 4-axial Turn-Milling

4. Conclusion

(1) Dither in orthogonal 4-axial turn-milling by end mill with eccentricity is influenced by geometrical shape of end mill, frequency response function of machine-tool's structure in three direction and property of workpiece's material, besides, it is relevant closely to cutting depth and rotating speed of mill.

(2) Frequency of dither's occurrence is close to main mode of system, analysis of cutting force spectrum shows forced frequency of main shaft or cutting-in frequency of cutter tooth. Value of cutting force and surface roughness is a multiple of value in the condition of un-dither, even it is dozen times more.

(3) Accuracy of theoretical model and simulating results are verified by analysis of cutting force spectrum and measurement of workpiece's surface roughness in orthogonal 4-axial turn-milling by end mill. Thus, rational cutting parameters can avoid dither effectively in machining and provide theoretical guidance for improvement of surface quality of workpiece and efficiency of machining.

Acknowledgments

This work is sponsored by the Hunan Science and Technology Division province funded projects (2013GK3028), and the project of Hunan province department of education(13C179).

References

[1] J. Chunde and J. Zenghui, "Vector modeling of orthogonal turn-milling movement and theoretical analysis on roughness of surface", Chinese Journal of Mechanical Engineering, vol. 37, no. 3, **(2001)**, pp. 62-64.
[2] S. Skoric, T. Udiljak and D. Ciglar, "Study of the suitability of the machining of rotating surfaces", Transactions of Famena, vol. 32, no. 2, **(2008)**, pp. 69-83.
[3] S. K. Choudhury and J. B. Bajpai, "Investigation in orthogonal turn-milling towards better surface finish", Journal of Materials Processing Technology, vol. 170, no. 3, **(2005)**, pp. 487-493.
[4] Y. Guan, H. Guan and G. Wang, "The modeling of cuttting force in high-speed milling for end mill", Sensors & Transducer, vol. 8, **(2014)**, pp. 210-217.
[5] E. Sabahudin, B. Edin and S. Amira, "Comparison of machined surface quality obtained by high-speed machining and conventional turning", Machining Science and Technology, vol. 11, **(2007)**, pp. 531-551.
[6] J. Zenghui and J. Chunde, "Theoretical cutting force of non-eccentricity orthogonal turn-milling", Chinese Journal of Mechanical Engineering, vol. 42, no. 9, **(2006)**, pp. 23-28.
[7] Z. Lida, "Study on simulation and experiment of turn-milling mechanism and dynamic characteristics", Shenyang: Northeastern University, **(2010)**.
[8] Y. Altintas, "Analytical prediction of three dimensional chatter stability in milling", JSME International Journal, vol. 44, no. 3, **(2001)**, pp. 717-723.
[9] Y. Altintas, G. Stepan and D. Merdol, "Chatter stability of milling in frequency and discrete time domain", Annals of the CIRP, vol. 53, no. 1, **(2008)**, pp. 35-44.
[10] E. Shamoto and K. Akazawa, "Analytical prediction of chatter stability in ball end milling with tool inclination", CIRP Annals-Manufacturing Technology, vol. 58, **(2009)**, pp. 351-354.
[11] M. Pogacink and J. Kopac, "Dynamic stabilization of the turn-milling process by parameter optimization", Proc. Instn. Mech. Engrs., vol. 214, **(2000)**, pp. 127-135.
[12] A. Schubert, A. Nestler and R. Funke, "Influence of cutting edge geometry and cutting parameters on surface finish in turn-milling of aluminum matrix composites", Mater. Wis. Werkstofftech., vol. 41, **(2010)**, pp. 795-801.
[13] S. Qinghua, W. Yi and A. Xing, "Novel method for dynamic optimization of stability in high-speed milling system", Transactions of Nanjing University of Aeronautics &Astronautics, vol. 26, **(2009)**, pp. 184-191.
[14] W. Tongyue, H. Ning and L. Liang, "Vibration model in milling of thin-walled components", Chinese Journal of Mechanical Engineering, vol. 43, no. 8, **(2007)**, pp. 22-25.
[15] L. Zhongqun and L. Qiang, "Modeling and simulation of chatter stability for circular milling", Journal of Mechanical Engineering, vol. 46, no. 4, **(2010)**, pp. 181-186.
[16] T. Aijun and L. Zhanqiang, "Perspectives and progress in three-dimensional stability lobes in milling chatter system", Tool Engineering, vol. 5, **(2008)**, pp. 3-5.
[17] S. Li, C. Ertao and J. Zenghui, "Test analysis on vibration signal of thin aluminium-alloy cylinder machined with orthogonal turn-milling", Acta Armamentarii, vol. 3, **(2009)**, pp. 356-360.
[18] F. Dongju, Z. Fuling and X. Zhanguo, "Mathematic model of material removal rate for ultrasonic milling", China Mechanical Engineering, vol. 17, no. 13, **(2006)**, pp. 1399-1403.
[19] W. Qua, K. Wanga and M. H. Miller, "Using vibration-assisted grinding to reduce subsurface damage", Precision Engineering, vol. 24, **(2000)**, pp. 329-337.

Author

Yue qi Guan, associate professor, research on CAD/CAM of surface processing for complex curve.

